A Pilot Study of ^{68}Ga-PSMA11 and ^{68}Ga-RM2 PET/MRI for Evaluation of Prostate Cancer Response to High-Intensity Focused Ultrasound Therapy

Heying Duan[1], Pejman Ghanouni[2], Bruce Daniel[2], Jarrett Rosenberg[1], Guido A. Davidzon[1], Carina Mari Aparici[1], Christian Kunder[3], Geoffrey A. Sonn[2,4], and Andrei Iagaru[1]

[1]Division of Nuclear Medicine and Molecular Imaging, Department of Radiology, Stanford University, Stanford, California; [2]Division of Body MRI, Department of Radiology, Stanford University, Stanford, California; [3]Department of Pathology, Stanford University, Stanford, California; and [4]Department of Urology, Stanford University, Stanford, California

Focal therapy for localized prostate cancer (PC) using high-intensity focused ultrasound (HIFU) is gaining in popularity as it is noninvasive and associated with fewer side effects than standard whole-gland treatments. However, better methods to evaluate response to HIFU ablation are an unmet need. Prostate-specific membrane antigen (PSMA) and gastrin-releasing peptide receptors are both overexpressed in PC. In this study, we evaluated a novel approach of using both ^{68}Ga-RM2 and ^{68}Ga-PSMA11 PET/MRI in each patient before and after HIFU to assess the accuracy of target tumor localization and response to treatment. **Methods:** Fourteen men, 64.5 ± 8.0 y old (range, 48–78 y), with newly diagnosed PC were prospectively enrolled. Before HIFU, the patients underwent prostate biopsy, multiparametric MRI, ^{68}Ga-PSMA11, and ^{68}Ga-RM2 PET/MRI. Response to treatment was assessed at a minimum of 6 mo after HIFU with prostate biopsy (n = 13), as well as ^{68}Ga-PSMA11 and ^{68}Ga-RM2 PET/MRI (n = 14). The SUV_{max} and SUV_{peak} of known or suspected PC lesions were collected. **Results:** Pre-HIFU biopsy revealed 18 cancers, of which 14 were clinically significant (Gleason score ≥ 3 + 4). Multiparametric MRI identified 18 lesions; 14 of them were at least score 4 in the Prostate Imaging–Reporting and Data System. ^{68}Ga-PSMA11 and ^{68}Ga-RM2 PET/MRI each showed 23 positive intraprostatic lesions; 21 were congruent in 13 patients, and 5 were incongruent in 5 patients. Before HIFU, ^{68}Ga-PSMA11 identified all target tumors, whereas ^{68}Ga-RM2 PET/MRI missed 2 tumors. After HIFU, ^{68}Ga-RM2 and ^{68}Ga-PSMA11 PET/MRI both identified clinically significant residual disease in 1 patient. Three significant ipsilateral recurrent lesions were identified, whereas 1 was missed by ^{68}Ga-PSMA11. The pretreatment level of prostate-specific antigen decreased significantly after HIFU, by 66%. Concordantly, the pretreatment SUV_{max} decreased significantly after HIFU for ^{68}Ga-PSMA11 (P = 0.001) and ^{68}Ga-RM2 (P = 0.005). **Conclusion:** This pilot study showed that ^{68}Ga-PSMA11 and ^{68}Ga-RM2 PET/MRI identified the target tumor for HIFU in 100% and 86% of cases, respectively, and accurately verified response to treatment. PET may be a useful tool in the guidance and monitoring of treatment success in patients receiving focal therapy for PC. These preliminary findings warrant larger studies for validation.

Key Words: ^{68}Ga-RM2; ^{68}Ga-PSMA11; PET; prostate cancer; HIFU

J Nucl Med 2023; 64:592–597
DOI: 10.2967/jnumed.122.264783

Standard treatment options for localized prostate cancer (PC) include active surveillance, radical prostatectomy, radiation (with or without hormonal therapy), and local therapy. Focal ablation is particularly of interest as whole-gland treatment with surgery or radiation may cause adverse events such as incontinence, impotence, and bowel or bladder dysfunction. These side effects may adversely impact the patients' quality of life (*1–4*). High-intensity focused ultrasound (HIFU) is a noninvasive local treatment that uses thermal energy to ablate low-risk PC lesions. Recently published data from large multicenter studies reported minimal impact on quality of life, with preservation of continence in 98% and of sexual function in 90% (*5*), and a 7-y failure-free survival rate of 69% (*6*). However, there is a 20%–40% rate of residual disease or relapse, requiring repeat HIFU. Treatment evaluation is an unmet need as there are no noninvasive, validated methods to assess success or failure (*7*). Posttreatment serum prostate-specific antigen (PSA) is a poor measure as it falls to a variable nadir due to continued production by residual prostate. The Phoenix criterion for biochemical failures after radiation therapy is commonly used after HIFU; however, it has poor sensitivity and specificity of only 65% and 77%, respectively (*8*). The subsequently introduced Stuttgart definition is specific for patients treated with HIFU and defines biochemical failure as the PSA nadir plus 1.2 ng/mL (*9*). The use of multiparametric MRI (mpMRI) for HIFU treatment assessment is impeded by signal alteration due to scar tissue, focal hemorrhage, and central necrosis (*10–13*). Therefore, posttreatment prostate biopsy remains the most accurate tool to evaluate treatment outcome but is invasive and includes significant risks such as pain, bleeding, and infection (*14,15*).

PET combined with MRI using radiopharmaceuticals that target prostate-specific membrane antigen (PSMA) or gastrin-releasing peptide receptors (GRPR)—both are overexpressed on PC cells—have been evaluated for staging and biochemical recurrence of PC. It may also be a useful technique to evaluate treatment outcome after HIFU. The effect of HIFU on the expression of PSMA or GRPR has not been investigated yet. In this study, we evaluated a novel approach using both ^{68}Ga-RM2 and ^{68}Ga-PSMA11 PET/MRI in each PC patient before and at a minimum of 6 mo after HIFU to assess the accuracy of target tumor localization and response to treatment.

MATERIALS AND METHODS

Participants

Participants with newly diagnosed PC scheduled to undergo HIFU were prospectively enrolled and scanned with ^{68}Ga-PSMA11 followed

Received Aug. 9, 2022; revision accepted Oct. 27, 2022.
For correspondence or reprints, contact Andrei Iagaru (aiagaru@stanford.edu).
Published online Nov. 3, 2022.

by ^{68}Ga-RM2 PET/MRI within 2 wk, or vice versa. The local institutional review board approved this Health Insurance Portability and Accountability Act–compliant study (NCT03949517). All patients gave written informed consent. The participants' clinical characteristics before treatment are shown in Table 1.

PET/MRI Protocol

Imaging was performed using a 3-T time-of-flight–enabled PET/MRI scanner (Signa; GE Healthcare), as previously described (*16,17*). The pre-HIFU image acquisition started at 46.50 ± 3.50 min (range, 44.00–57.00 min) after injection of 151.33 ± 44.80 MBq (range, 70.30–222.00 MBq) of ^{68}Ga-PSMA11 and at 45.50 ± 2.12 min (range, 43.00–52.00 min) after injection of 138.80 ± 4.61 MBq (range, 132.98–150.20 MBq) of ^{68}Ga-RM2. Simultaneous PET/MRI was acquired from vertex to mid thigh with an acquisition time of 4 min per bed position for an overall scan length of 49.00 ± 16.96 min (range, 30.00–83.00 min) for ^{68}Ga-PSMA11 and 47.00 ± 6.58 min (range, 36.00–60.00 min) for ^{68}Ga-RM2. The PET/MRI examinations included a dedicated 20-min pelvic acquisition. These images were acquired after a delay of 23.00 ± 9.19 min (range, 22.00–49.00 min) for ^{68}Ga-PSMA11 and 25.00 ± 5.54 min (range, 11.00–37.00 min) for ^{68}Ga-RM2. The PET/MRI scans were performed 5.50 ± 2.50 d (range, 2.00–9.00 d) apart. The syntheses of ^{68}Ga-PSMA11 and ^{68}Ga-RM2 were previously described (*18*). The post-HIFU ^{68}Ga-PSMA11 and ^{68}Ga-RM2 image acquisition details were similar to pretreatment imaging (Table 2).

TABLE 1
Patients' Characteristics Before HIFU Ablation

Characteristic	Data
n	14
Age (y)	64.50 ± 8.00 (48.00–78.00)
PSA (ng/mL)	8.41 ± 3.47 (1.22–15.90)
PSA density (ng/mL^2)	0.23 ± 0.09 (0.07–0.31)
mpMRI	18 lesions
PI-RADS 5	3 (17%)
PI-RADS 4	11 (61%)
PI-RADS 3	4 (22%)
Biopsy, Gleason grade	18 lesions
1	3 (17%)
2	5 (28%)
3	7 (39%)
4	2 (11%)
5	1 (5%)
Risk	
Intermediate	13
High	1
Clinical stage	
T1c	5
T2a	2
T2b	4
T2c	3
^{68}Ga-PSMA11	
Injected activity (MBq)	151.33 ± 44.80 (70.30–222.00)
Uptake time (min)	46.50 ± 3.50 (44.00–57.00)
Length of PET/MRI (min)	49.00 ± 16.96 (30.00–83.00)
Delay to pelvic PET/MRI (min)	23.00 ± 9.19 (22.00–49.00)
^{68}Ga-RM2	
Injected activity (MBq)	138.80 ± 4.61 (132.98–150.20)
Uptake time (min)	45.50 ± 2.12 (43.00–52.00)
Length of PET/MRI (min)	47.00 ± 6.58 (36.00–60.00)
Delay to pelvic PET/MRI (min)	25.00 ± 5.54 (11.00–37.00)
Time between scans (d)	5.50 ± 2.50 (2.00–9.00)

Qualitative data are number and percentage; continuous data are median ± SD and range.

mpMRI Protocol

All mpMRI was performed as routine clinical scans before and 1 y after HIFU using a 3-T scanner (MR750; GE Healthcare) with an external 32-channel body array coil. The imaging protocol consisted

TABLE 2
Patients' Characteristics After HIFU Ablation

Characteristic	Data
n	14
PSA (ng/mL)	2.83 ± 1.65 (0.02–5.79)
PSA density (ng/mL^2)	0.07 ± 0.04 (0.00–0.17)
PSA nadir (ng/mL)	2.80 ± 1.48 (0.01–5.79)
Time to PSA nadir (mo)	6.55 ± 5.92 (2.90–24.83)
Biopsy (*n* = 13)	
Residual lesions	
Clinically significant	1
Clinically insignificant	3
Recurrent lesions	
Clinically significant	3
Clinically insignificant	6
^{68}Ga-PSMA11	
Injected activity (MBq)	145.60 ± 37.75 (82.51–221.26)
Uptake time (min)	47.50 ± 2.40 (41.00–49.00)
Length of PET/MRI (min)	45.50 ± 5.90 (33.00–62.00)
Delay to pelvic PET/MRI (min)	26.00 ± 6.53 (22.00–48.00)
^{68}Ga-RM2	
Injected activity (MBq)	139.77 ± 5.04 (133.32–149.67)
Uptake time (min)	46.00 ± 3.14 (39.00–52.00)
Length of PET/MRI (min)	51.50 ± 9.53 (41.00–73.00)
Delay to pelvic PET/MRI (min)	26.00 ± 6.22 (21.00–47.00)
Time between scans (d)	5.00 ± 40.66 (2.00–172.00)
Time between pre- and post-HIFU scans (mo)	7.43 ± 2.37 (5.93–12.60)

Qualitative data are number and percentage; continuous data are median ± SD and range.

of T2-weighted, diffusion-weighted, and dynamic contrast-enhanced sequences. The acquisition parameters were previously described in detail (*19*). The target tumor for HIFU treatment was determined on mpMRI and defined as having a Prostate Imaging–Reporting and Data System (PI-RADS) score of at least 4 and clinically significant PC (csPC) on biopsy (Gleason score ≥ 3 + 4).

Image Analysis

Two nuclear medicine physicians, experienced in interpreting PSMA- and GRPR-targeted molecular imaging, reviewed and analyzed the PET images independently, in random order, and masked to the clinical results. A consensus reading was performed for discordant findings. The framework from the PROMISE criteria was used for PSMA PET interpretation. Focal uptake of ^{68}Ga-RM2 or ^{68}Ga-PSMA11 above the adjacent prostate background and not associated with physiologic accumulation was recorded as suggestive of PC. A region of interest was drawn over suspected lesions to measure SUV_{max} and SUV_{peak}. SUV_{peak} is defined as the average SUV within a small, fixed-size region of interest (1 cm^3).

mpMRI was analyzed using the PI-RADS criteria, version 2 (*20*). Lesions with a PI-RADS score of at least 3 were recorded. A PI-RADS score of 3 was considered equivocal for PC, PI-RADS 4 likely for PC, and PI-RADS 5 highly likely for PC.

HIFU

Focal HIFU ablation of localized PC was performed with curative intent using the Sonablate device (Sonacare Medical). One target tumor was treated per patient. Treated areas included the MRI lesion with an 8- to 10-mm margin of normal surrounding tissue. The follow-up included PSA and follow-up visits every 3 mo and mpMRI and biopsy at 1 y.

Prostate Biopsy

Prostate biopsy was performed under local anesthesia using MRI–ultrasound fusion and included targeted sampling of the treated zone, any MRI lesions, and standard-template 12-core biopsy with 1 core through the apex, mid, and base regions, both medially and laterally, from the left and right prostate lobes (*21,22*).

Statistical Analysis

Statistical analysis was performed using Stata, version 16.1 (StataCorp LP), and R, version 4.1.1 (r-project.org). Continuous data are presented as median ± SD, range, and interquartile range. Comparison between biopsy-positive and biopsy-negative regions of PI-RADS, ^{68}Ga-PSMA11, and ^{68}Ga-RM2 (SUV_{max}), and between SUV_{max} and SUV_{peak} for whole-body and delayed pelvic imaging before and after HIFU ablation, was done by the Wilcoxon rank sum test, adjusted for clustering. A P value of less than 0.05 was considered significant. Sensitivity and specificity (adjusted for clustering) were calculated using a segment-based approach in which the prostate was divided into the same 12 segments as for systematic prostate biopsy. The segments were dichotomized according to the pathologic findings from biopsy. Values are given as percentages with 95% CIs.

RESULTS

Fourteen men 64.5 ± 8.0 y old (range, 48–78 y) with newly diagnosed PC and scheduled to undergo HIFU were prospectively enrolled. Tables 1 and 2 summarize pre- and post-HIFU patient characteristics, respectively.

PSA and PSA Density

PSA and PSA density before HIFU ablation were 8.41 ± 3.47 ng/mL (range, 1.22–15.90 ng/mL) and 0.23 ± 0.09 ng/mL^2 (range, 0.07–0.31 ng/mL^2), respectively. At posttreatment PET imaging, 7.43 ± 2.37 mo (range, 5.93–12.60 mo) after HIFU, PSA and PSA density decreased by 66% to 2.83 ± 1.65 ng/mL (range, 0.02–5.79 ng/mL) ($P = 0.001$) and 0.07 ± 0.04 ng/mL^2 (range, 0.00–0.17 ng/mL^2) ($P = 0.001$), respectively. A PSA nadir of 2.80 ± 1.48 ng/mL (range, 0.01–5.79 ng/mL) was found at 6.55 ± 5.92 mo (range, 2.90–24.83 mo) after treatment.

mpMRI

Routine clinical pre-HIFU mpMRI identified 18 lesions (3 PI-RADS 5, 11 PI-RADS 4, and 4 PI-RADS 3). The dominant csPC lesion was treated with HIFU. The sensitivity and specificity of pre-HIFU mpMRI were 43% and 98%, respectively. After treatment, routine mpMRI was available for 13 participants because 1 patient was lost to follow-up 1 y after HIFU: 9 of 13 patients were negative, and 4 of 13 patients had a PI-RADS 3 lesion. One of these 4 correlated to residual Gleason 4 + 4 disease (mpMRI also identified 2 pathologic lymph nodes), 2 correlated to Gleason 3 + 3 residual lesions (not identified on PET because of urinoma), and 1 was benign on post-HIFU biopsy. One PI-RADS 4 lesion in the same participant was benign on biopsy as well. Significant ipsilateral ($n = 3$) and contralateral ($n = 6$) recurrences were all missed by mpMRI (negative scan). A direct comparison of mpMRI, ^{68}Ga-PSMA11, and ^{68}Ga-RM2 PET/MRI is shown in Table 3.

TABLE 3
Direct Comparison of mpMRI, ^{68}Ga-PSMA11, and ^{68}Ga-RM2 PET/MRI Findings Before and After HIFU Ablation

	mpMRI		^{68}Ga-PSMA11		^{68}Ga-RM2	
Parameter	Before HIFU	After HIFU	Before HIFU	After HIFU	Before HIFU	After HIFU
All lesions (*n*)	18 (PI-RADS 3: 4; PI-RADS 4: 11; PI-RADS 5: 3)	5 (PI-RADS 3: 4; PI-RADS 4: 1)	23	9 (2 residual; 7 recurrent)	23	9 (1 residual; 8 recurrent)
Target lesions	14	9/13 patients: negative; 3/13 patients: PI-RADS 3 (1 csPC, 2 ncsPC)	14	2 residual (1 csPC; 2 ncsPC)	12	1 residual (1 csPC)
Sensitivity	43%		81%		70%	
Specificity	98%		89%		88%	

TABLE 4
SUV_{max} and SUV_{peak} of Target Lesions in Whole Body and Delayed Pelvic ^{68}Ga-PSMA11 and ^{68}Ga-RM2 PET/MRI Before and After HIFU Ablation

	^{68}Ga-PSMA11		^{68}Ga-RM2	
Parameter	Whole body	Delayed pelvic	Whole body	Delayed pelvic
Before HIFU, SUV_{max}	9.51 (6.63–18.50)	8.91 (6.66–18.94)	7.70 (5.67–11.05)	7.48 (4.97–11.51)
After HIFU				
SUV_{max}	2.27 (1.80–2.78)	2.03 (1.80–2.51)	2.55 (2.07–3.48)	2.61 (1.68–2.74)
P	0.001	0.001	0.005	0.006
Before HIFU, SUV_{peak}	5.04 (3.97–8.84)	5.16 (4.27–9.50)	5.22 (4.15–8.05)	4.96 (4.02–8.57)
After HIFU				
SUV_{peak}	1.96 (1.89–2.31)	2.11 (1.83–2.39)	3.06 (2.85–3.49)	2.81 (2.22–3.08)
P	0.012	0.068	0.026	0.084

Data are median and interquartile range.

Prostate Biopsy

Before HIFU, prostate biopsies showed 18 lesions, of which 14 were csPC with a Gleason score of at least 3 + 4 and were determined to be target tumors for HIFU ablation. After treatment, prostate biopsy was available for 13 participants: Residual disease was detected in 4 patients: 1 was csPC with Gleason 4 + 4 (identified on both ^{68}Ga-PSMA11 and ^{68}Ga-RM2 PET/MRI), and 3 were Gleason 3 + 3 cancers (2/3 not seen on PET because of urinoma, 1/3 identified with ^{68}Ga-PSMA11 but missed on ^{68}Ga-RM2 PET/MRI). Outside the treated area, 3 ipsilateral Gleason 4 + 3 recurrences were found in 3 patients (2/3 seen with both radiopharmaceuticals, 1/3 missed by ^{68}Ga-PSMA11 but positive on ^{68}Ga-RM2) and subsequently received HIFU. Nonaggressive recurrence contralaterally was detected in 6 patients (1 lesion each was missed by either radiopharmaceutical in 2 different patients, the rest were identified with both ^{68}Ga-PSMA11 and ^{68}Ga-RM2 PET/MRI); 3 of these 6 lesions were known from pre-HIFU biopsy.

^{68}Ga-PSMA11 PET/MRI

Pre-HIFU ^{68}Ga-PSMA11 PET/MRI showed 23 intraprostatic lesions; all 14 target tumors for HIFU were correctly identified. Other positive lesions correlated to non–clinically significant PC (ncsPC) ($n = 4$) or high-grade prostatic intraepithelial neoplasia ($n = 3$) from pre-HIFU prostate biopsy. The sensitivity and specificity of pre-HIFU ^{68}Ga-PSMA11 PET/MRI were 81% and 89%, respectively. After HIFU ablation, ^{68}Ga-PSMA11 PET/MRI identified 9 lesions, which correlated to residual csPC ($n = 1$) and ncsPC ($n = 1$) and recurrent ipsilateral csPC ($n = 2$) and contralateral ncsPC ($n = 5$). The SUV_{max} from whole-body and dedicated pelvic imaging decreased significantly after HIFU, whereas SUV_{peak} showed significance only in the whole-body images. Table 4 summarizes all SUVs.

^{68}Ga-RM2 PET/MRI

The pre-HIFU ^{68}Ga-RM2 PET/MRI also showed 23 intraprostatic lesions, of which 12 of 14 (85.7%) target tumors for HIFU were identified. Other positive lesions correlated to ncsPC ($n = 4$), high-grade prostatic intraepithelial neoplasia ($n = 3$), and atypical small acinar proliferation suggestive of but nondiagnostic for PC ($n = 1$) in pre-HIFU biopsies. The sensitivity and specificity of pre-HIFU ^{68}Ga-RM2 PET/MRI were 70% and 88%, respectively. After HIFU, ^{68}Ga-RM2 PET/MRI also identified 9 lesions, which correlated to residual csPC ($n = 1$), recurrent ipsilateral csPC ($n = 3$), and contralateral ncsPC ($n = 5$). Concordant with ^{68}Ga-PSMA11 PET, the SUV_{max} from whole-body and dedicated pelvic images decreased significantly after HIFU, whereas SUV_{peak} was significant only for the whole-body images (Table 4).

Comparison Between ^{68}Ga-PSMA11 and ^{68}Ga-RM2

Before HIFU, ^{68}Ga-PSMA11 and ^{68}Ga-RM2 PET/MRI were concordant in 21 of 23 lesions in 14 patients and discordant in 5 lesions in 5 patients. Except for the 2 target tumors missed by ^{68}Ga-RM2 PET, all target tumors were congruent (Fig. 1). Incongruent lesions correlated to atypical small acinar proliferation ($n = 1$) and false-positive uptake ($n = 2$) in pre-HIFU biopsy. After HIFU, ^{68}Ga-PSMA11 and ^{68}Ga-RM2 PET/MRI showed concordant uptake in a Gleason 4 + 4 residual lesion. In this participant, pretreatment ^{68}Ga-PSMA11 identified a positive pelvic lymph node that was subsequently treated with stereotactic body radiation therapy. On the posttreatment ^{68}Ga-PSMA11 PET, this lymph node showed resolution, but 2 new pelvic lymph nodes were identified; all were all negative on ^{68}Ga-RM2 PET. ^{68}Ga-RM2 PET also missed 1 nonsignificant residual lesion seen on ^{68}Ga-PSMA11, whereas ^{68}Ga-PSMA11 missed 1 recurrent csPC lesion identified on ^{68}Ga-RM2 PET. Both radiopharmaceuticals showed congruent uptake in 2 ipsilateral recurrent csPC lesions, which were treated with HIFU. Nonsignificant contralateral recurrent disease showed congruency in 4 patients, of which 3 were already seen in the pre-HIFU biopsies and were positive on both pretreatment scans. ^{68}Ga-PSMA11 missed a nonaggressive recurrence, which was seen on ^{68}Ga-RM2 PET, and vice versa in another patient. Two nonsignificant residual lesions were missed by both radiopharmaceuticals because of an adjacent urinoma. There were no false-positive findings on post-HIFU PET.

DISCUSSION

In this era driven by precise, personalized medicine, interest is growing in noninvasive, targeted, focal treatment of csPC lesions using HIFU, and adoption is widening. We hypothesized that noninvasive PET/MRI assessment of response to HIFU may be a useful tool. The effect of HIFU on PSMA- and GRPR-overexpressing PC

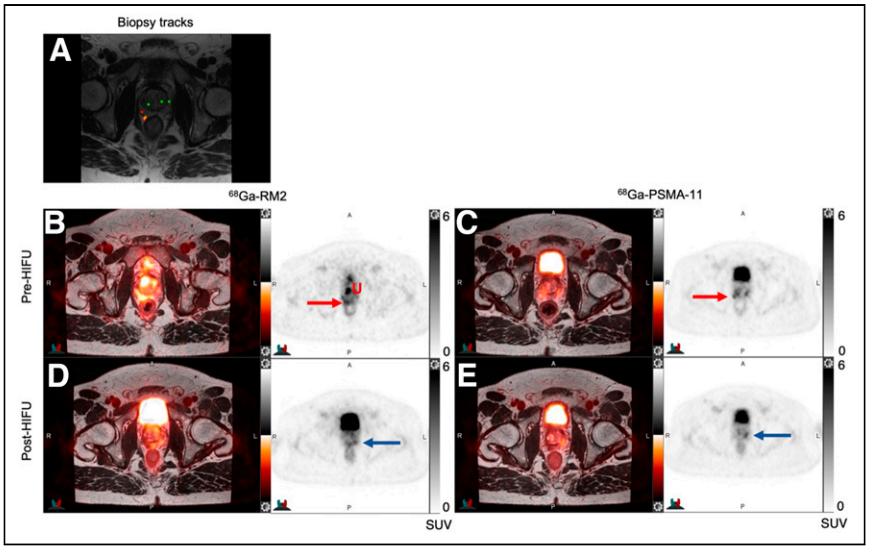

FIGURE 1. A 62-y-old man with Gleason 3 + 4 PC in right lateral base and Gleason 3 + 3 PC in right posterior base (A shows color-coded needle tracks from biopsy; green: benign, yellow: Gleason 3 + 3, red: Gleason ≥ 3 + 4). He presented with PSA of 7.0 ng/mL and PSA density of 0.24 ng/mL^2. Pretherapy ^{68}Ga-RM2 (B) and ^{68}Ga-PSMA-11 (C) axial PET/MRI and PET, respectively, show focal uptake in right prostate lesion (red arrows). This was treated with HIFU, and 6 mo later, uptake resolved on ^{68}Ga-RM2 (D) and ^{68}Ga-PSMA11 (E) axial PET/MRI and PET, respectively. Focal uptake in left prostate (blue arrows) was subsequently biopsied and showed nonaggressive PC. U = urethra with excreted ^{68}Ga-RM2.

cells has not been investigated yet in a direct comparison. This prospective study showed that ^{68}Ga-RM2 and ^{68}Ga-PSMA11 PET/MRI are feasible for identification of the target lesion for HIFU, as well as for evaluation of treatment success. Therefore, repeated invasive prostate biopsies after HIFU may be avoided in some men.

Burger et al. were the first to evaluate a very specific subgroup of patients with residual csPC on biopsy but negative mpMRI results after HIFU with ^{68}Ga-PSMA11 PET/MRI (*23*). Six of the 10 patients were positive on ^{68}Ga-PSMA11, without any false-positives. The sensitivity, specificity, and positive and negative predictive values were 55%, 100%, 100%, and 85%, respectively. The authors concluded that ^{68}Ga-PSMA11 PET/MRI may be able to detect residual PC not seen on mpMRI after HIFU but acknowledged the risk of false-negative ^{68}Ga-PSMA11 PET results. In our study, both ^{68}Ga-PSMA11 and ^{68}Ga-RM2 accurately identified the only patient with residual csPC. ^{68}Ga-PSMA11 also detected 1 patient with nonaggressive residual disease, missed on ^{68}Ga-RM2. Because our patient cohort consisted mostly of those with negative mpMRI findings, and those negative for or with nonaggressive residual PC after HIFU, no direct comparison can be made between the studies. There are no other studies evaluating the use of ^{68}Ga-PSMA11 or ^{68}Ga-RM2 PET to guide or evaluate focal treatment of PC.

Before HIFU, ^{68}Ga-PSMA11 and ^{68}Ga-RM2 PET/MRI identified the target tumor in 100% and 86% of cases, respectively. These results are comparable to recently published detection rates of 98% and 95% for ^{68}Ga-PSMA11 and ^{68}Ga-RM2, respectively, in patients with newly diagnosed PC correlated with postprostatectomy pathologic findings (*24*). Most PET-positive lesions were concordant between the 2 radiopharmaceuticals. The discordant uptake pattern reflects the difference in expression pattern between PSMA and GRPR, which has previously been reported by our group (*17,24,25*) and is supported by immunohistochemistry analyses (*26*), suggesting that PSMA- and GRPR-targeting radiopharmaceuticals may be complementary to each other. mpMRI was equivocal in 2 residual ncsPC lesions that PET missed, whereas the csPC residual and ipsilateral recurrent disease was missed by mpMRI. The only PI-RADS 4 lesion correlated to benign prostatic tissue in posttreatment biopsy. The post-HIFU mpMRI interpretation is impeded by signal alteration of the treated area, whereas ipsilateral recurrence is particularly difficult to read because of potential focal hemorrhage, edema, scar tissue, and central necrosis (*10–13*).

In the interpretation of post-HIFU ^{68}Ga-PSMA11 and ^{68}Ga-RM2 PET/MRI, we observed an intense PET signal correlating to or associated with a widened urethral lumen on the accompanying MRI, which could be "pulled" toward the treated area, most likely because of scar tissue formation after ablation. This has been previously described by Kirkham et al. as "capacious prostatic cavity continuous with the urethra" (*11*) and is similar to the change in prostate appearance after transurethral resection (*27*). This finding suggests that PET/MRI may be better suited to evaluate HIFU treatment outcome than mpMRI and PET/CT because of high soft-tissue contrast and thus better delineation of structural changes and distinguishing of urinoma with excreted radiotracer from true residual tumor or ipsilateral recurrence.

The patients with Gleason 4 + 3 recurrence subsequently underwent HIFU ablation. This additional finding suggests that ^{68}Ga-PSMA11 and ^{68}Ga-RM2 PET/MRI may also play a role in delineating recurrent lesions for HIFU retreatment and therefore in guiding patient management after HIFU.

PSA decreased significantly after HIFU by 66% within 7 mo, and the PSA nadir occurred at 6.5 mo. These results are consistent with other studies reporting that the median time to the PSA nadir after HIFU varied from 3 to 12 mo, with a PSA reduction of between 53% and 84% (*28–31*).

Focal therapies aim to address patients who fall between active surveillance and radical whole-gland treatment. Finding a cutoff for when to treat with which modality remains difficult. No clear guidelines exist on optimal candidates for HIFU, as long-term results are still lacking. The most recent consensus, from 2017 (*32*), suggests HIFU for localized disease with low to intermediate risk; however, more recent trends favor active surveillance over treatment for low-risk cancers. One interesting finding in our study was the patient who showed metastatic disease before treatment but progression after HIFU. This suggests that HIFU is not suitable for metastasized-PC patients and supports the importance of molecular whole-body imaging.

Our study had 3 noteworthy limitations. The first was the small number of patients. This is common in pilot studies. Second, 1 participant lacked posttreatment biopsy and mpMRI, as he is still awaiting his 1-y follow-up. Delays in patient care due to the study's being conducted during the coronavirus disease 2019 pandemic resulted in a wider time span of post-HIFU evaluations than originally planned. Third, the relatively short follow-up after HIFU

prevented us from investigating the correlation of signal loss on ^{68}Ga-RM2 and ^{68}Ga-PSMA11 PET with long-term outcome. However, the encouraging data presented here warrant larger studies investigating the role of ^{68}Ga-RM2 and ^{68}Ga-PSMA11 PET/MRI in focal-therapy patient selection, treatment planning, and follow-up evaluation.

CONCLUSION

In this pilot study, ^{68}Ga-PSMA11 and ^{68}Ga-RM2 PET/MRI identified the dominant lesion for HIFU ablation in 100% and 86% of cases, respectively, and accurately verified response to treatment. Clinically significant residual disease and ipsilateral recurrences were accurately identified by both radiopharmaceuticals. PET may be a useful tool in the guidance and monitoring of treatment success in patients receiving focal therapy. Further evaluation in larger cohorts is needed to validate these results.

DISCLOSURE

The study was partially supported by GE Healthcare. No other potential conflict of interest relevant to this article was reported.

KEY POINTS

QUESTION: Is the use of ^{68}Ga-PSMA11 and ^{68}Ga-RM2 PET/MRI feasible to identify the target tumor for HIFU and assess treatment success in patients with intermediate-risk PC?

PERTINENT FINDINGS: ^{68}Ga-PSMA11 and ^{68}Ga-RM2 PET/MRI identified the target tumor for HIFU ablation in 100% and 86% of cases, respectively. Clinically significant residual disease and ipsilateral recurrences were accurately identified by both radiopharmaceuticals. ^{68}Ga-PSMA11 additionally detected lymph node metastases, which ultimately changed patient management.

IMPLICATIONS FOR PATIENT CARE: Use of ^{68}Ga-PSMA11 and ^{68}Ga-RM2 PET/MRI was feasible for monitoring HIFU treatment success and may avoid repeated biopsies for treatment verification.

REFERENCES

1. Nepple KG, Stephenson AJ, Kallogjeri D, et al. Mortality after prostate cancer treatment with radical prostatectomy, external-beam radiation therapy, or brachytherapy in men without comorbidity. *Eur Urol.* 2013;64:372–378.
2. Hamdy FC, Donovan JL, Lane JA, et al. 10-year outcomes after monitoring, surgery, or radiotherapy for localized prostate cancer. *N Engl J Med.* 2016;375:1415–1424.
3. Barocas DA, Alvarez J, Resnick MJ, et al. Association between radiation therapy, surgery, or observation for localized prostate cancer and patient-reported outcomes after 3 years. *JAMA.* 2017;317:1126–1140.
4. Capogrosso P, Vertosick EA, Benfante NE, et al. Are we improving erectile function recovery after radical prostatectomy? analysis of patients treated over the last decade. *Eur Urol.* 2019;75:221–228.
5. Lovegrove CE, Peters M, Guillaumier S, et al. Evaluation of functional outcomes after a second focal high-intensity focused ultrasonography (HIFU) procedure in men with primary localized, non-metastatic prostate cancer: results from the HIFU Evaluation and Assessment of Treatment (HEAT) registry. *BJU Int.* 2020;125:853–860.
6. Reddy D, Peters M, Shah TT, et al. Cancer control outcomes following focal therapy using high-intensity focused ultrasound in 1379 men with nonmetastatic prostate cancer: a multi-institute 15-year experience. *Eur Urol.* 2022;81:407–413.
7. Barret E, Harvey-Bryan KA, Sanchez-Salas R, Rozet F, Galiano M, Cathelineau X. How to diagnose and treat focal therapy failure and recurrence? *Curr Opin Urol.* 2014;24:241–246.
8. Roach M III, Hanks G, Thames H Jr, et al. Defining biochemical failure following radiotherapy with or without hormonal therapy in men with clinically localized prostate cancer: recommendations of the RTOG-ASTRO Phoenix Consensus Conference. *Int J Radiat Oncol Biol Phys.* 2006;65:965–974.
9. Blana A, Brown SC, Chaussy C, et al. High-intensity focused ultrasound for prostate cancer: comparative definitions of biochemical failure. *BJU Int.* 2009;104:1058–1062.
10. Rouvière O, Lyonnet D, Raudrant A, et al. MRI appearance of prostate following transrectal HIFU ablation of localized cancer. *Eur Urol.* 2001;40:265–274.
11. Kirkham AP, Emberton M, Hoh IM, Illing RO, Freeman AA, Allen C. MR imaging of prostate after treatment with high-intensity focused ultrasound. *Radiology.* 2008;246:833–844.
12. Rosenkrantz AB, Taneja SS. Radiologist, be aware: ten pitfalls that confound the interpretation of multiparametric prostate MRI. *AJR.* 2014;202:109–120.
13. Rouvière O, Girouin N, Glas L, et al. Prostate cancer transrectal HIFU ablation: detection of local recurrences using T2-weighted and dynamic contrast-enhanced MRI. *Eur Radiol.* 2010;20:48–55.
14. Tay KJ, Amin MB, Ghai S, et al. Surveillance after prostate focal therapy. *World J Urol.* 2019;37:397–407.
15. Loeb S, Vellekoop A, Ahmed HU, et al. Systematic review of complications of prostate biopsy. *Eur Urol.* 2013;64:876–892.
16. Duan H, Baratto L, Hatami N, et al. Reduced acquisition time per bed position for PET/MRI using ^{68}Ga-RM2 or ^{68}Ga-PSMA-11 in patients with prostate cancer: a retrospective analysis. *AJR.* 2022;218:333–340.
17. Minamimoto R, Hancock S, Schneider B, et al. Pilot comparison of ^{68}Ga-RM2 PET and ^{68}Ga-PSMA-11 PET in patients with biochemically recurrent prostate cancer. *J Nucl Med.* 2016;57:557–562.
18. Minamimoto R, Sonni I, Hancock S, et al. Prospective evaluation of ^{68}Ga-RM2 PET/MRI in patients with biochemical recurrence of prostate cancer and negative findings on conventional imaging. *J Nucl Med.* 2018;59:803–808.
19. Sonn GA, Fan RE, Ghanouni P, et al. Prostate magnetic resonance imaging interpretation varies substantially across radiologists. *Eur Urol Focus.* 2019;5:592–599.
20. Weinreb JC, Barentsz JO, Choyke PL, et al. PI-RADS prostate imaging–reporting and data system: 2015, version 2. *Eur Urol.* 2016;69:16–40.
21. Heidenreich A, Bastian PJ, Bellmunt J, et al. EAU guidelines on prostate cancer. Part 1: screening, diagnosis, and local treatment with curative intent—update 2013. *Eur Urol.* 2014;65:124–137.
22. Wolf AM, Wender RC, Etzioni RB, et al. American Cancer Society guideline for the early detection of prostate cancer: update 2010. *CA Cancer J Clin.* 2010;60:70–98.
23. Burger IA, Muller J, Donati OF, et al. ^{68}Ga-PSMA-11 PET/MR detects local recurrence occult on mpMRI in prostate cancer patients after HIFU. *J Nucl Med.* 2019;60:1118–1123.
24. Duan H, Baratto L, Fan RE, et al. Correlation of ^{68}Ga-RM2 PET with postsurgery histopathology findings in patients with newly diagnosed intermediate- or high-risk prostate cancer. *J Nucl Med.* 2022;63:1829–1835.
25. Baratto L, Song H, Duan H, et al. PSMA- and GRPR-targeted PET: results from 50 patients with biochemically recurrent prostate cancer. *J Nucl Med.* 2021;62:1545–1549.
26. Touijer KA, Michaud L, Alvarez HAV, et al. Prospective study of the radiolabeled GRPR antagonist BAY86-7548 for positron emission tomography/computed tomography imaging of newly diagnosed prostate cancer. *Eur Urol Oncol.* 2019;2:166–173.
27. Sheu MH, Chiang H, Wang JH, Chang YH, Chang CY. Transurethral resection of the prostate-related changes in the prostate gland: correlation of MRI and histopathology. *J Comput Assist Tomogr.* 2000;24:596–599.
28. Dickinson L, Ahmed HU, Hindley RG, et al. Prostate-specific antigen vs. magnetic resonance imaging parameters for assessing oncological outcomes after high intensity-focused ultrasound focal therapy for localized prostate cancer. *Urol Oncol.* 2017;35:30.e9–30.e15.
29. Chapelon JY, Rouviere O, Crouzet S, Gelet A. Prostate focused ultrasound therapy. *Adv Exp Med Biol.* 2016;880:21–41.
30. Rischmann P, Gelet A, Riche B, et al. Focal high intensity focused ultrasound of unilateral localized prostate cancer: a prospective multicentric hemiablation study of 111 patients. *Eur Urol.* 2017;71:267–273.
31. Ahmed HU, Dickinson L, Charman S, et al. Focal ablation targeted to the index lesion in multifocal localised prostate cancer: a prospective development study. *Eur Urol.* 2015;68:927–936.
32. Tay KJ, Scheltema MJ, Ahmed HU, et al. Patient selection for prostate focal therapy in the era of active surveillance: an international Delphi consensus project. *Prostate Cancer Prostatic Dis.* 2017;20:294–299.